Uncertainty Estimation of Human-Exoskeleton Interaction Using a Robotic Dummy

1st Stefano Massardi
DIMI,University of Brescia
Brescia, Italy

BioRobotics Group
Centre for Automation and Robotics (CAR),CSIC-UPM, Madrid, Spain
(stefano.massardi@unibs.it)

2nd David Rodriguez-Cianca
BioRobotics Group
Centre for Automation and Robotics (CAR),CSIC-UPM, Madrid, Spain

3rd Diego Torricelli
BioRobotics Group
Centre for Automation and Robotics (CAR),CSIC-UPM, Madrid, Spain

4th Matteo Lancini
DSMC
University of Brescia
Brescia, Italy

***Abstract*—Exoskeletons and exosuits have witnessed unprecedented growth in recent years, especially in the medical and industrial sectors. The study of human-exoskeleton interaction relies on the participation of potential exoskeleton users, which gives rise to safety concerns and substantial testing resources. Specifically, the study of physical human-exoskeleton interaction (pHEI) is based on several metrics that are typically challenging to assess in a systematic way. To address this, we present an instrumented setup composed of a mechatronic leg able to sense interaction forces, together with a vision system for measuring pHEI kinematic metrics. In this study, we started from a previously designed protocol to extract key metrics utilized in assessing pHEI, such as joint misalignments, relative motions and interaction forces. Subsequently, we carried out an uncertainty analysis on these chosen metrics of interest. To achieve this, a series of experiments were conducted to assess the influence of the measurement uncertainty on each metric through multiple test repetitions. Despite generally acceptable uncertainty values, angular misalignment metrics warrant further investigation since their associated uncertainty is close to the value of its standard deviation in the conditions tested. These findings emphasize the importance of conducting such an analysis, offering insights for the future measurement protocols verification and improvements.**

***Index Terms*—physical human-exoskeleton interaction, exoskeletons, wearable robots**

I. Introduction

Exoskeletons are wearable devices that enhance the subject's movement and/or motor skills by applying forces to the limbs through physical interfaces [1]. These robotic exoskeletons are widely used in various sectors including: i) healthcare, where they serve as a tool for mobilizing impaired limbs during rehabilitation therapies [2], ii) personal assistance, aimed at aiding the movement of individuals with mobility issues [3], iii) industry, where they are used to improve ergonomics and minimize worker injuries during repetitive tasks [4], and iv) military, with the objective of augmenting human physical capabilities [5]. Furthermore, the demand for exoskeletons is increasing every year, driven by the increase of population's aging, neurological injuries like stroke, and a growing prevalence of mobility impairments [6].

A special attention should be given to exoskeletons considering their close interaction with users. Their potential to safely transmit power to the user via coupling force is limited by their kinematic incompatibilities with the user [7]. These incompatibilities arise because exoskeletons usually have fewer degrees of freedom than humans. Therefore, ensuring correct fitting and alignment is crucial to prevent joints misalignments, and consequently relative movements between the exoskeleton frame and the user's limbs [8]. Joint misalignments refer to the offsets between the centers of rotation of two mechanically connected bodies. These misalignments can arise during the initial joint alignment phase when the device is worn or due to drifts in the device's position over the user's body [9]. For these reasons, a proper exoskeleton fitting and alignment is crucial since incorrect positioning can lead to undesired interaction forces and affect joint load [10]. Developers must consider hazards associated with misalignments (both translational and rotational) during exoskeleton design. In a recent survey it was highlighted how misalignments are a matter of general concern across the wearable robot community [11]. Nevertheless, although research on pHEI is still limited, joint misalignments have received significant attention from the scientific community. Specifically, joint misalignments and relative motions were found to represent the key kinematic metrics for pHEI assessment [12].

However, only a very limited portion of this literature addresses how effectively the selected metrics can be measured in the specific working scenario. Typically, joint misalignments and relative motions are monitored using vision system that tracks the device's position on the user. This approach enables the direct extraction of the relative position between the human and exoskeleton [13], or the validation of predictive models for human-exoskeleton positions [14], [15]. In other cases, device alignment is verified either with a meter or based on visual feedback from the operator. In the case of vision systems, a marker-based model can be employed to extract joint centers of rotation and relative displacements. However, precision and accuracy of these measurements are

rarely considered in this field, as well as their impact on the results. These models often involve a computational step where joint centers are calculated based on geometric considerations. These additional computations can introduce more uncertainty into the measurements, due to the accuracy of the system assessing the individual markers positions, the calculations, and to the geometrical approximations used. How these affect the selected analysis is then mostly unexplored. Specifically, research on robotic exoskeletons significantly lacks uncertainty analysis, with only a few studies addressing it in human motion analysis, which is the primary application area for vision systems [16], [17].

In this work we considered a measuring system capable of recording both pHEI kinematic and kinetic metrics. The core of the system is based on a mechatronic replica of a human leg, composed of a human-like actuation system at the knee level and an anthropomorphic sensorized surface able to measure interaction forces in the three dimensions. This prototype enables the execution of reproducible experiments. A camera based vision system is added for the extraction of the kinematic metrics related with pHEI. Within this system, we considered a marker-based model to extract joint misalignments and relative motions. We performed an uncertainty budget for the kinematic metrics used to evaluate misalignment in different conditions. Multiple experiments are then conducted under the same conditions to quantify the metrics variance across trials. We then selected an indicator to quantify the measurement quality. The outcome will reveal whether this system and protocol are effective in measuring the considered metrics and whether the variability in results is associated with the underlying phenomena or the measurement uncertainty.

II. Materials and Method

A. Experimental setup

In this study, we adopted the experimental setup described in [18], utilizing a mechatronic dummy leg known as the Leg Replica introduced in [19]. This dummy leg was specifically designed to mimic the anatomical characteristics, dimensions, weight, inertia, and movement patterns of a real human leg. The knee joint of the Leg Replica features an actuated hinge mechanism that allows for precise position control in the sagittal plane. The hip and ankle joints are designed as passive ball joints capable of being locked into predetermined spatial orientations. To monitor interaction forces at a detailed level, the Leg Replica is equipped with eight triaxial load cells positioned beneath its external surface—four in the thigh segment and four in the shank segment (see Fig. 1a). Each segment includes four 3D-printed ABS material surface shells, distributed between the front and back sides, with each shell connected to a load cell. This setup facilitates the measurement of net interaction forces applied to each surface shell. The inclusion of this setup ensures precise measurement of interaction forces at the physical interfaces (exoskeleton cuffs), enhancing experimental repeatability and control—an aspect often challenging in human trials. Additionally, a soft layer resembling human soft tissues is applied to the Leg Replica's surface, following the guidelines outlined in ISO/TR23482-1 [20]. Specifically, we selected a silicon-based material (EcoFlex 00-30 Smooth-On) with a shear modulus consistent with typical values found in biological tissues [21]. This material was adhered to both the thigh and lower shank portions of the Leg Replica. To capture kinematic data related to the interaction, a motion capture system (VICON, Oxford) is employed around the Leg Replica. In our experiments, the Leg Replica is fitted with a 1-degree-of-freedom (1-DOF) knee exoskeleton prototype featuring three cuffs (two at the thigh level and one at the shank level).

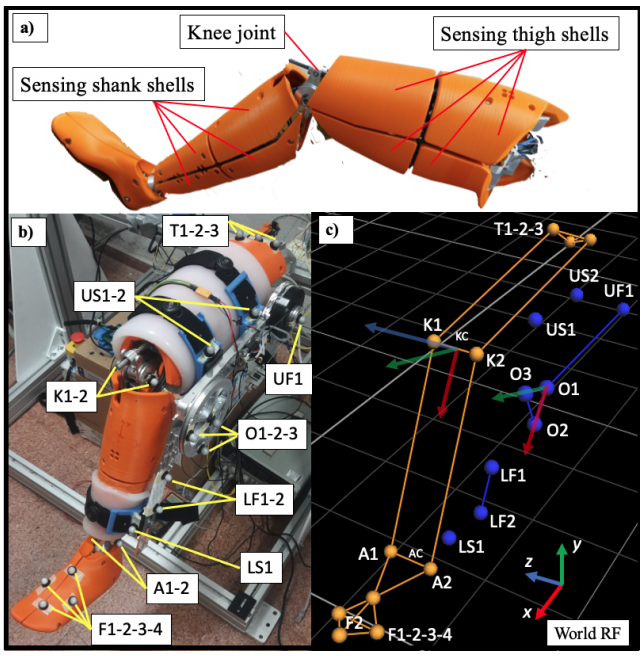

Fig. 1. The setup and protocol replicated from [18]. (a) Lateral view of the Leg Replica prototype and its sensing surface shells. (b) Knee exoskeleton attached to the Leg Replica, including reflective markers grouped by name (c) Leg replica's marker models, with marker labels and reference systems for the leg and knee exoskeleton. Markers were placed on the upper leg straps (US1, US2), upper exoskeleton frame (UF1), knee joint (O1, O2, O3) lower leg strap (LS1), lower exoskeleton frame (LF1, LF2), leg thigh (T1, T2, T3), leg knee hinge (K1, K2), leg ankle (A1, A2) and foot (F1, F2, F3, F4). World and local reference frames follow the following convention: x=red, y=green, z=blue

B. Kinematic metrics computation

To quantify relative motions and misalignments between the exoskeleton and the Leg Replica, we built a marker-based protocol as depicted in Figure 1c. In this protocol, virtual markers are computed for the leg's ankle joint center (AC) and the leg's knee joint center (KC). These markers represent the midpoint of segments A1A2 and K1K2, respectively. The knee reference frame (KRF) is established with its origin at KC. The x-axis aligns with KCAC, the z-axis corresponds to KCK1, while the y-axis results from the vector product of the other two axes. Similarly, the exoskeleton knee joint reference frame (ERF) is determined. Its origin lies at point O1 (located at the exoskeleton's pulley center of rotation). The x-axis passes through O2 (on the pulley's circumference, aligned with the

exoskeleton lower frame), while the y-axis intersects O3 (also on the pulley's circumference, positioned at a 90-degree angle from O2). To mitigate unwanted occlusion effects, K1 and K2 markers are reconstructed relative to a fixed reference frame (RF) created from markers T1, T2, and T3. Similarly, markers A1 and A2 are calculated based on a fixed RF located on the foot (markers F1, F2, and F3). After building KRF and ERF frames, the kinematic metrics can be computed:

- Spatial misalignment (Mx, My) [mm]: Offset in the XY plane between the axis of rotation of the Leg Replica's knee joint and that of the exoskeleton knee joint, i.e., x-y offset between the position of marker KC and marker O1 of Fig. 1b.
- Angular misalignemnt (αx,αy,αz) [deg]: Angular offset between the 2 reference frames KRF and ERF.
- Relative displacement (dx,dy,dz) [mm]: Relative position of the exoskeleton cuff with respect to the leg. Computed as the position of marker LS1 in KRF coordinates.

C. Test protocol

A series of experiments were performed to examine the impact of the uncertainty in measurements on the variability of the outcomes. The exoskeleton was attached to the Leg Replica in two distinct misalignment setups. One is referred to as "aligned", where the center of the ERF coincides with the KRF. The other referred as "misaligned", in which the center of the exoskeleton's pulley is shifted towards the hip of the leg, resulting in a misaligned coupling. The test consisted in imposing the Leg Replica to follow a sinusoidal position reference in the range 5-65deg for 60 seconds, with a frequency of 0.2 Hz, while recording kinematic and kinetic metrics. Throughout the movement, the exoskeleton remained transparent, i.e., it is fully backdrivable. Once the movement completed, the exoskeleton was detached and then reinstalled on the leg. Each condition is tested 15 times, with efforts made to ensure each runs are as identical as possible.

D. Metrics

To assess the quality of the measurements, we chose an indicator defined by the ratio of the metric's uncertainty to its variability observed in the conducted experiments. A lower ratio suggests effective measurement of the phenomena, while its variability is attributed to the phenomena itself. Conversely, with a higher ratio it is unclear whether the observed variability is due to the phenomena or from the inadequate accuracy in measuring the metric. Metrics' variability is computed by its standard deviation computed on the conducted trials. Metrics' uncertainty is estimated using a Montecarlo Method [22] starting from the single marker position's uncertainty, which is declared by the VICON software. This uncertainty is propagated in the operations needed to compute the selected metrics. A test was executed consisting in one 60 second run following the protocol as detailed in II-C. A Montecarlo method was applied to the data. For every frame each marker's coordinate was perturbed 1000 times following a normal distribution with σ taken as the highest marker uncertainty declared by the software after the standard VICON calibration procedure (σ=0.2 mm) and centered on the actual estimate (μ=0 mm). The metrics of interests are computed on the perturbated dataset and metrics' uncertainty resulted from their standard deviation.

III. Results

The calculated uncertainty associated with the kinematic and kinetic metrics along the three axes is collected in Table I. Kinematic metrics calculated from VICON exhibit different levels of uncertainty based on the axis along which they are computed. The uncertainty associated with force metrics remains constant, as it is directly derived from the characteristics of the sensors.

TABLE I
METRICS UNCERTAINTY

Metric	**x-axis**	**y-axis**	**z-axis**
Angle knee misalignment γ [deg]	2.7	2.7	0.8
Spacial knee misalignment M_x, M_y, zex [mm]	0.6	0.5	0.8
Cuff's relative displacement d [mm]	2.0	2.0	1.7
Interaction force F [N]	2.0	2.0	2.0

The ratio between the uncertainty of kinematic metrics and their standard deviation across the trials is displayed in Table II for metrics computed using the VICON system. Additionally, this ratio is further divided for trials conducted under both aligned and misaligned conditions. Notably, the misaligned condition generally exhibits a higher ratio compared to the aligned condition. For angle misalignment, the ratio surpasses a value of 1 for both the x and y axes. In the case of relative displacements, the ratio tends to hover around 50%. However, for spatial misalignment, it remains averagely contained.

TABLE II
RATIO U/SD OF KINEMATIC METRICS. RESULTS ON DIFFERENT AXIS ARE DIVIDED ON ALIGNED (A) AND MISALIGNED (M) TRIALS

Metric	**x-axis**		**y-axis**		**z-axis**	
	A	**M**	**A**	**M**	**A**	**M**
Angle knee misalignment γ	0.86	1.1	1.7	1.8	0.47	0.56
Spacial knee misalignment M_x, M_y, zex	0.26	0.55	0.14	0.13	0.13	0.1
Cuff's relative displacement d	0.47	0.56	0.49	0.58	0.52	0.72

Table III for kinetic metrics related to forces measured by the leg replica.

TABLE III
RATIO U/SD OF FORCE METRICS. RESULTS ON DIFFERENT AXIS ARE DIVIDED ON ALIGNED (A) AND MISALIGNED (M) TRIALS

Metric	**Upper Leg**		**Lower Leg**	
	A	**M**	**A**	**M**
Initial compression force Fc	0.16	0.16	0.16	0.16
Max tangential force Ft	0.28	0.09	0.2	0.08

IV. Discussion

This study presented an instrumental setup for measuring key metrics related to pHEI. For each of these metrics, we calculated the associated measurement uncertainty. The uncertainty associated with force metrics depends on the load cell installed in the dummy. Kinematic metrics were derived from mathematical computations based on the spacial coordinates of the reflective markers used in our VICON model. Optical systems (i.e. VICON) typically rely on the initial camera calibration performed according to the manufacturer's instructions. In the case of VICON system, a specific calibration procedure provides the spatial uncertainty of the single marker position estimated from each camera. Within this procedure, achieving a declared uncertainty from 0.1 mm to 0.2 mm can be generally straightforward. However, how the markers' position coordinates are combined and used in calculations can significantly impact the uncertainty associated with the considered metric measurement. The results presented in this work serve as concrete evidence of the importance of including an uncertainty analysis in such tests. The impact of this work is particularly significant given that exoskeleton-related studies typically lack of any uncertainty analysis. The measurement uncertainty associated with the kinematic metrics varied sensitively depending on the metric and the axis of computation. Trials were repeated in aligned and misaligned case by moving the exoskeleton along the x-axis. Spatial misalignment and relative displacement reached an acceptable level in terms of u/SD ratio suggesting that the system is sufficiently good to ensure the quality of these measurements. Trials conducted under misalignment conditions typically exhibited similar or higher u/SD ratios compared to aligned conditions, primarily due to the reduced deviation achieved during the exoskeleton positioning phase. This outcome was unintended but arose from the manual adjustment of the exoskeleton on the leg. Specifically, a u/SD ratio greater than 1.0 raises concerns about the reliability of the entire system. When this ratio is less than 1.0, the influence of the system is reduced, but there is still a noticeable contribution. Ratios less than 1.0 are considered acceptable, although ideally, u/SD ratios would be less than 0.5. The ratio results for the angle misalignments were sensitively higher compared with the other metrics and was found to be greater than 1 in three conditions. This outcome may be attributed to our initial estimation of uncertainty, which can vary from the actual uncertainty encountered. The word error from the VICON system consists of two components: a stochastic contribution related to the moving point, and a systematic contribution arising from the origin reference. Given that the markers are positioned closely on the leg, it follows that the position uncertainty of a marker relative to the VICON origin is likely higher than the position uncertainty from one marker to another. Our approach leads then to an overestimation, assuming that the proximity of the markers in our protocol does not reduce the initial uncertainty declared by the VICON system. Our overestimation could arises from the inhomogeneity of the measurement volume, suggesting that accuracy should not be assumed constant throughout the entire volume [17]. We then applied a "worse-case" scenario where we assumed constant uncertainty during calibration, due to the challenges involved in analyzing whether uncertainty was consistent across the entire volume. This factor could explain the elevated ratios observed for angular misalignment, which also coincides with the metric requiring more computational load and utilizing reference systems based on closely spaced markers. In future tests, this factor can be taken into account by adjusting the VICON origin according to the chosen marker protocol. For instance, differently from human gait analysis, a protocol using closely spaced markers should incorporate a reference system positioned nearby and implement a calibration procedure focused on a limited area. Regarding the force metrics considered, the resulting ratios indicated that the deviation was fully derived from the phenomena and was changing from trial to trial. These results indicate that we may have overestimated the measurement uncertainty associated with the kinematic metrics. While these uncertainty values remain acceptable for the main metrics under consideration, special attention should be given when dealing with angular misalignment, as this metric warrants further clarification.

V. Conclusion

This study underscores the importance of rigorously assessing uncertainty in both force and kinematic metrics in the field of pHEI. While force metrics exhibit stability attributed to the load cell, kinematic metrics are subject to variability influenced by marker computations in the VICON system. Despite generally acceptable uncertainty levels, the elevated ratios observed for angular misalignment metrics necessitate potential refinement of the measurement protocols. By highlighting the significance of uncertainty analysis in exoskeleton research, this study provides valuable insights for enhancing the reliability and interpretability of experimental findings in the field of biomechanics and rehabilitation engineering.

Acknowledgment

This work was supported by the project EXOSAFE, awarded by the COVR European Project under grant agreement No. 779966.

References

[1] A. J. Young and D. P. Ferris, "State of the art and future directions for lower limb robotic exoskeletons," *IEEE Transactions on Neural Systems and Rehabilitation Engineering*, vol. 25, no. 2, pp. 171–182, 2016.

[2] L. Jørgensen, B. Jacobsen, T. Wilsgaard, and J. Magnus, "Walking after stroke: does it matter? changes in bone mineral density within the first 12 months after stroke. a longitudinal study," *Osteoporosis international*, vol. 11, pp. 381–387, 2000.

[3] L. N. Awad, A. Esquenazi, G. E. Francisco, K. J. Nolan, and A. Jayaraman, "The rewalk restore™ soft robotic exosuit: a multi-site clinical trial of the safety, reliability, and feasibility of exosuit-augmented post-stroke gait rehabilitation," *Journal of neuroengineering and rehabilitation*, vol. 17, pp. 1–11, 2020.

[4] J. P. Pinho, C. Taira, P. Parik-Americano, L. O. Suplino, V. P. Bartholomeu, V. N. Hartmann, G. S. Umemura, and A. Forner-Cordero, "A comparison between three commercially available exoskeletons in the automotive industry: An electromyographic pilot study," in *2020 8th IEEE RAS/EMBS International Conference for Biomedical Robotics and Biomechatronics (BioRob)*. IEEE, 2020, pp. 246–251.

[5] D. J. Farris, D. J. Harris, H. M. Rice, J. Campbell, A. Weare, D. Risius, N. Armstrong, and M. P. Rayson, "A systematic literature review of evidence for the use of assistive exoskeletons in defence and security use cases," *Ergonomics*, vol. 66, no. 1, pp. 61–87, 2023.

[6] M. Mahdavian, A. G. Toudeshki, and A. Yousefi-Koma, "Design and fabrication of a 3dof upper limb exoskeleton," in *2015 3rd RSI international conference on robotics and mechatronics (ICROM)*. IEEE, 2015, pp. 342–346.

[7] J. L. Pons, *Wearable robots: biomechatronic exoskeletons*. John Wiley & Sons, 2008.

[8] A. T. Asbeck, S. M. De Rossi, K. G. Holt, and C. J. Walsh, "A biologically inspired soft exosuit for walking assistance," *The International Journal of Robotics Research*, vol. 34, no. 6, pp. 744–762, 2015.

[9] D. Zanotto, Y. Akiyama, P. Stegall, and S. K. Agrawal, "Knee joint misalignment in exoskeletons for the lower extremities: Effects on user's gait," *IEEE Transactions on Robotics*, vol. 31, no. 4, pp. 978–987, 2015.

[10] V. Bartenbach, D. Wyss, D. Seuret, and R. Riener, "A lower limb exoskeleton research platform to investigate human-robot interaction," in *2015 IEEE international conference on rehabilitation robotics (ICORR)*. IEEE, 2015, pp. 600–605.

[11] S. Massardi, D. Pinto-Fernandez, J. Babič, M. Dežman, A. Trošt, V. Grosu, D. Lefeber, C. Rodriguez, J. Bessler, L. Schaake *et al.*, "Relevance of hazards in exoskeleton applications: a survey-based enquiry," *Journal of NeuroEngineering and Rehabilitation*, vol. 20, no. 1, pp. 1–13, 2023.

[12] S. Massardi, D. Rodriguez-Cianca, D. Pinto-Fernandez, J. C. Moreno, M. Lancini, and D. Torricelli, "Characterization and evaluation of human–exoskeleton interaction dynamics: a review," *Sensors*, vol. 22, no. 11, p. 3993, 2022.

[13] Y. Akiyama, Y. Yamada, and S. Okamoto, "Interaction forces beneath cuffs of physical assistant robots and their motion-based estimation," *Advanced Robotics*, vol. 29, no. 20, pp. 1315–1329, 2015.

[14] D. Torricelli, C. Cortés, N. Lete, Á. Bertelsen, J. E. Gonzalez-Vargas, A. J. Del-Ama, I. Dimbwadyo, J. C. Moreno, J. Florez, and J. L. Pons, "A subject-specific kinematic model to predict human motion in exoskeleton-assisted gait," *Frontiers in neurorobotics*, vol. 12, p. 18, 2018.

[15] C. Cortés, A. Ardanza, F. Molina-Rueda, A. Cuesta-Gomez, L. Unzueta, G. Epelde, O. E. Ruiz, A. De Mauro, J. Florez *et al.*, "Upper limb posture estimation in robotic and virtual reality-based rehabilitation," *BioMed research international*, vol. 2014, 2014.

[16] F. Crenna, G. B. Rossi, and A. Palazzo, "Measurement of human movement under metrological controlled conditions," *Acta Imeko*, vol. 4, no. 4, pp. 48–56, 2015.

[17] P. Eichelberger, M. Ferraro, U. Minder, T. Denton, A. Blasimann, F. Krause, and H. Baur, "Analysis of accuracy in optical motion capture–a protocol for laboratory setup evaluation," *Journal of biomechanics*, vol. 49, no. 10, pp. 2085–2088, 2016.

[18] S. Massardi, D. Rodriguez-Cianca, M. Cenciarini, D. C. Costa, J. M. Font-Llagunes, J. C. Moreno, M. Lancini, and D. Torricelli, "Systematic evaluation of a knee exoskeleton misalignment compensation mechanism using a robotic dummy leg," in *2023 International Conference on Rehabilitation Robotics (ICORR)*. IEEE, 2023, pp. 1–6.

[19] M. Dežman, S. Massardi, D. Pinto-Fernandez, V. Grosu, C. Rodriguez-Guerrero, J. Babič, and D. Torricelli, "A mechatronic leg replica to benchmark human–exoskeleton physical interactions," *Bioinspiration & Biomimetics*, vol. 18, no. 3, p. 036009, 2023.

[20] "ISO/TR 23482-1:2020 Robotics — Application of ISO 13482 — Part 1: Safety-related test methods," International Organization for Standardization, Technical Report, Feb. 2020.

[21] J. L. Sparks, N. A. Vavalle, K. E. Kasting, B. Long, M. L. Tanaka, P. A. Sanger, K. Schnell, and T. A. Conner-Kerr, "Use of silicone materials to simulate tissue biomechanics as related to deep tissue injury," *Advances in skin & wound care*, vol. 28, no. 2, pp. 59–68, 2015.

[22] JCGM 101:2008, "Evaluation of measurement data – supplement 1 to the guide to the expression of uncertainty in measurement – propagation of distributions using a monte carlo method," 2008.